

Micromagnetic investigation of current-driven magnetic excitation in a spin valve structure

This article has been downloaded from IOPscience. Please scroll down to see the full text article.

2007 J. Phys.: Condens. Matter 19 165211

(<http://iopscience.iop.org/0953-8984/19/16/165211>)

View [the table of contents for this issue](#), or go to the [journal homepage](#) for more

Download details:

IP Address: 129.252.86.83

The article was downloaded on 28/05/2010 at 17:51

Please note that [terms and conditions apply](#).

Micromagnetic investigation of current-driven magnetic excitation in a spin valve structure

K J Lee

Department of Materials Science and Engineering, Korea University, Seoul, Korea

E-mail: kj_lee@korea.ac.kr

Received 22 September 2006, in final form 16 November 2006

Published 6 April 2007

Online at stacks.iop.org/JPhysCM/19/165211

Abstract

Using micromagnetic modelling we study current-driven magnetic dynamics in a spin valve structure. We take into account the Slonczewski's spin torque term and the Oersted field due to charge current. Special attention is paid to excitation of the incoherent spin-wave induced by the spin torque which significantly affects the switching current, switching time and telegraph noise. The incoherence is mainly due to spatial inhomogeneity of local magnetic fields, which generate a distribution of local precession frequencies. Here we show the main consequences of the incoherent spin-wave which provides a quantitative understanding of the experimental results on magnetic dynamics due to spin-transfer effects. We also discuss the limitations and perspectives of micromagnetic modelling for the current-driven dynamics.

1. Introduction

An electrical current excites magnetization in a nanomagnet when the incoming electrons are spin-polarized and the current density is sufficiently large to overcome the intrinsic Gilbert damping [1, 2]. The magnetic excitation due to a spin-polarized electrical current, i.e. spin-transfer torque (STT), has triggered lots of theoretical [3–7] and experimental studies [8–24] because of its great potential for new spintronic devices.

The STT is caused by the absorption of a transverse spin current in a nanomagnet. The STT is non-zero in a magnetic structure with non-collinear magnetizations where a part of the magnetizations provides a spin current transverse to another. A spin valve consisting of two ferromagnets separated by a non-magnet enables us to make a discrete change in the magnetizations along the direction of the current flow and is therefore an important structure for studying the spin transfer effect. The current-induced magnetization switching as a novel writing scheme for magnetic random access memory (MRAM) provides scalability below 100 nm. In the present write scheme of MRAM, field-driven magnetization switching, the write current increases on decreasing the cell area, whereas in current-induced magnetization

switching, it decreases on decreasing the cell area because it is determined by a critical current density.

The spin-torque theory was derived from the single domain assumption [1, 2]. The coherent spin-torque model describes the effect of the STT in terms of *uniform* rotation of the magnetization within the framework of the single domain Landau–Lifshitz–Gilbert (LLG) equation [5]. The coherent spin-torque model has been widely used to analyse experimental observations of the magnetic excitation due to the STT [5, 24–26]. However, it failed to explain some experimental results [20–22], and as a result, an alternative model was proposed: the effective magnetic temperature model. The effective magnetic temperature model describes the magnetic excitations in terms of the spin-flip scattering due to *non-uniform* magnons, effectively raising the magnetic temperature [27, 28].

An important controversy between the coherent spin-torque model and the effective magnetic temperature model was raised in interpreting telegraph noises [20, 21]. Telegraph noise is a consequence of random jumps between two stable states, i.e. parallel (P) and anti-parallel (AP) magnetic configurations in the spin valve structure. For instance, the energy barrier for an AP to P transition is much higher than that for a P to AP transition when the magnetic field preferring the P state is applied without current. In this case it is hard to create a situation where the relaxation time at the P state (τ_P) is similar to that at the AP state (τ_{AP}). This is because the residual time of magnetization at a state is exponentially proportional to the associated energy barrier. The only way of making the situation $\tau_P \sim \tau_{AP}$ by the field alone is to apply it along the hard axis. Even with the field applied along the easy axis, however, it is possible to make both relaxation times similar when the current is injected. When the current preferring the AP state is applied with the magnetic field preferring the P state, the energy barrier for the AP to P state transition effectively reduces due to the anti-damping effect of the STT so that the telegraph noise is observable in a reasonable timescale.

In the coherent spin-torque model, the residual time of thermally assisted magnetization switching between the two states was derived from a generalized stochastic LLG equation and its corresponding Fokker–Planck equation for the magnetization dynamics [26]:

$$\tau = f_0^{-1} \exp\left(\frac{E_B^0}{k_B T} \left(1 - \frac{I}{I_C^{\text{SDM}}}\right)\right) \quad (1)$$

$$I_C^{\text{SDM}} = \frac{2\gamma e S \alpha}{P} (H + H_K + 2\pi M_s) \quad (2)$$

where f_0 is the attempt frequency, E_B^0 is the energy barrier without current effects, k_B is the Boltzmann constant, T is the sample temperature, I is the current, I_C^{SDM} is the critical current for magnetic excitation in the single domain model, P is the spin polarization efficiency, γ is the gyromagnetic ratio, α is the intrinsic damping constant, S is the total spin, H is the external magnetic field, H_K is the anisotropy field, and M_s is the saturation magnetization.

Figure 1 shows a schematic phase diagram of the telegraph noise as a function of the current and the field under the single domain assumption. Two energy minima and the activation energy for magnetization fluctuations are preconditions for telegraph noise. In region I, there are two energy minima because both the field and the current are smaller than the critical values ($H_c =$ coercivity, $I_c =$ critical current corresponding to a_c). According to the coherent spin-torque model, magnetic hysteresis and telegraph noise can be observed only in region I. In region II, there is a single energy minimum because the current is larger than I_c whereas the field is smaller than H_c . In this region, the stable magnetic configuration is determined by the current. In contrast, it is determined by the field in region III where a single energy minimum is allowed. In region IV, only the precession motion is possible because both field and current are larger than the critical values, i.e. there is no energy minimum.

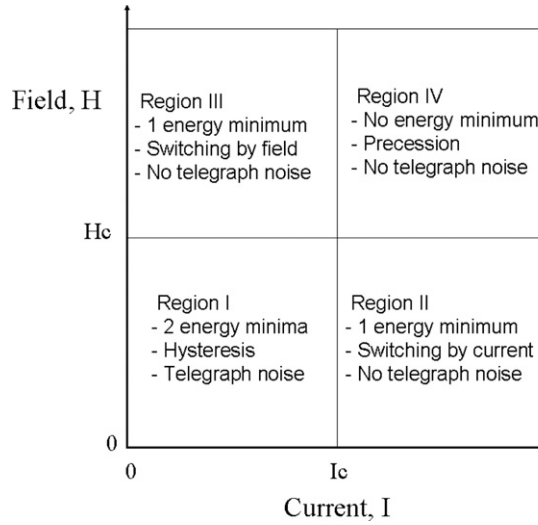


Figure 1. Schematic phase diagram of the coherent spin-torque model as a function of the current and the field. H_c is the coercivity and I_c is the critical current for the magnetic excitation.

Therefore, if the single domain assumption is valid, we can observe telegraph noise only in region I. However, Urazhdin *et al* [20] observed telegraph noise at a current larger than the critical value, which cannot be described within the framework of the coherent spin-torque model. This indicates that the magnetization could be inhomogeneous in the dynamics. A micromagnetic study including the STT term has shown that non-uniform magnetization [29] and chaotic behaviour [30, 31] can be caused by the STT. In this work we show that a main origin of the incoherence is the Oersted field due to the charge current. We discuss the main consequences of the incoherent dynamics and the way of suppressing the incoherence.

2. Model

As a good approximation, the effect of the spin-transfer torque can be captured by an additional term in the conventional LLG equation:

$$\frac{d\mathbf{M}}{dt} = -\gamma\mathbf{M} \times \mathbf{H}_{\text{eff}} + \frac{\alpha}{M_s}\mathbf{M} \times \frac{d\mathbf{M}}{dt} + \frac{\gamma a_J}{M_s}\mathbf{M} \times (\mathbf{M} \times \mathbf{p}). \quad (3)$$

The effective field \mathbf{H}_{eff} includes the crystalline anisotropy, the exchange, the magnetostatic and the external fields. The first term on the right-hand side of (3) is Slonczewski's expression of the spin-torque term [1]. Here, \mathbf{M} is the magnetization vector of the free layer, \mathbf{p} is a unit vector parallel to the electron polarization, and a_J is the amplitude of the spin torque in the unit of magnetic field. In this work, we did not take into account the angular dependence of a_J . Three types of sample were tested (samples 1 and 2 are shown in table 1). Sample 3 is also NiFe, but various sizes were tested [32]. The other assumptions were: collinear polarization of incoming electrons with the pinned layer magnetization set along the long axis, and no stray field from the pinned layer on the free layer; initially parallel magnetic configuration; and electrons flowing from the free to the pinned layer. In-plane external fields were applied along the long axis. Positive external fields prefer the parallel magnetic configuration. The current-induced magnetic field was included. We assumed an infinite current line to calculate the Oersted field and therefore the effect of the Oersted field is a bit exaggerated in our work.

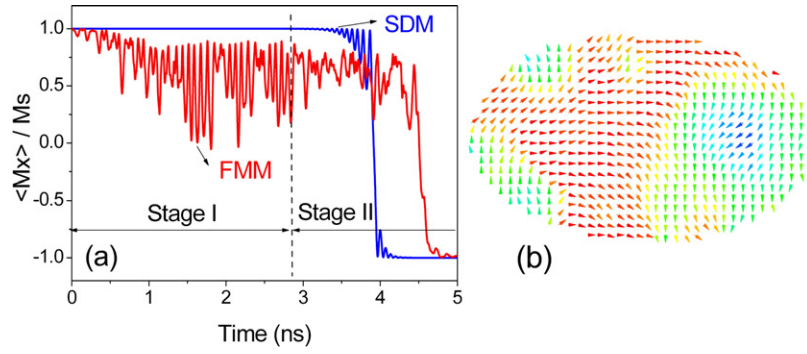


Figure 2. Magnetization switching due to the spin-transfer torque. (a) Spatially averaged magnetization (M_x) versus time at $I = -4$ mA and $H = 0$ Oe. (b) Typical chaotic domain pattern obtained at stage II (sample 1) [31].

(This figure is in colour only in the electronic version)

Table 1. Model parameters of the free layer of tested samples.

Parameters	Sample 1 (Co)	Sample 2 (NiFe)
Shape and size, $L \times W \times t$ (nm ³)	Ellipse, $130 \times 72 \times 3$	Rectangle, $64 \times 32 \times 3$
M_s (emu cm ⁻³)	1420	800
H_K (Oe)	30	15
Exchange constant, A (erg cm ⁻¹)	2.0×10^{-6}	1.0×10^{-6}
Intrinsic damping constant, α	0.014	0.02
a_J per mA (Oe)	77.7	118.6

This may change the bias condition for the incoherence but does not alter the main conclusion of this work. For the stochastic calculation, the Gaussian-distributed random fluctuation field (mean = 0, standard deviation = $\sqrt{2\alpha k_B T / (\gamma M_s V \Delta t)}$, where Δt is the integration time step, and V is the volume of unit cell) [33] has been added to the effective fields of the LLG equation.

3. Results and discussions

3.1. Incoherent spin-wave excitation [31]

As we reported in [31], the full micromagnetic model (FMM) shows a quite complex dynamics whereas the single domain model (SDM) shows that the spin-polarized current excites coherent precession modes which eventually lead to the magnetization switching (figure 2(a)). Before the switching in the FMM, two consecutive time stages showing quite different domain motions can be distinguished:

- (i) growth of the precessing end domains (stage I), and
- (ii) chaotic domain motion (stage II).

When the current is turned on, the magnetizations at the two long ends of the cell start to precess (stage I). Incoherent spin-waves are first excited at the long edges because of the Oersted field. Once the end domains have almost joined each other, the magnetizations at the centre of the cell start to precess (stage II). A growing spatial incoherency in the precession frequency and magnetization orientation is observed. It originates from the spatial

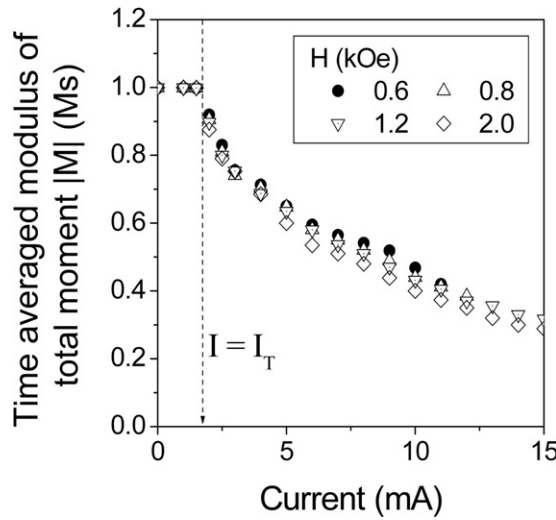


Figure 3. Time-averaged $|M|$ for 100 ns as a function of current (sample 1) [31].

non-uniformity of the local magnetic fields and magnetization orientation. Consequently, the domain motion becomes chaotic (stage II, figure 2(b)), and finally the magnetization switches.

The incoherent spin-wave excitation and chaotic dynamics were observed in a broad range of the current and the field. As shown in figure 3, the time-averaged modulus of the total moment $|M|$ is reduced from the saturation magnetization (M_s), indicating large-amplitude incoherent spin-wave excitation when $I > 2$ mA ($=I_T$: the current for the abrupt increase in the incoherence). We found that the magnetic dynamics is coherent at $I < I_T$, but the incoherence abruptly increases with current at $I > I_T$. The dependence of the incoherence versus I is found to be independent of the applied field over a wide range of field investigated, indicating that the current and therefore the STT solely determines the incoherence.

The large amplitude spin-waves observed in our work may be rather surprising because of too high magnetic (mostly exchange) energy. In this case, the spin current must be taken into account to estimate the total energy of the system and to check whether or not it obeys the conservation law. However, it was claimed that there is no well-defined energy associated with the spin current [26], indicating a difficulty to describe the spin current by an effective magnetic field, a derivative of the associated energy ($-\partial E/\partial \mathbf{M}$). Recalling that this argumentation is still under debate [34, 35], it is hard to verify our predictions of spin-wave frequencies and mode profile in terms of the conservation law. As shown in our previous paper [31], however, the simulated spectra are in a good agreement with ones measured by the Cornell group [19]. Furthermore, a recent experiment involving time-resolved x-ray imaging [36] showed the vortex formation during the current-induced magnetization switching as observed in the modelling study. These could be evidences to verify the validity of our modelling results.

3.2. Telegraph noise in region I ($I < I_c$ and $H < H_c$) and region II ($I > I_c$ and $H < H_c$)

In this section, we show the effect of the incoherent dynamics on the telegraph noise at room temperature. In both the SDM and the FMM, we could obtain telegraph noise (figures 4(a) and (b)). In the SDM, the theoretical prediction of (1) (solid lines in the figure 4(c)) is in an excellent agreement with the simulation results. We could not observe telegraph noise at $I > I_c$

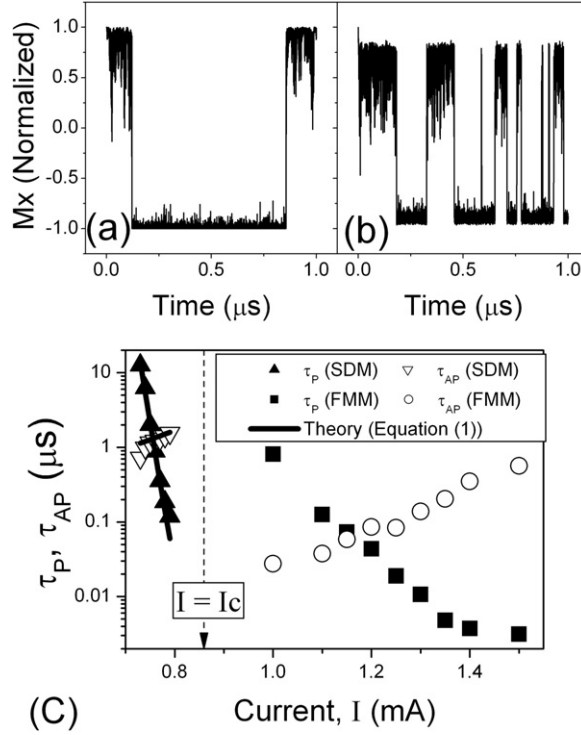


Figure 4. Telegraph noise of sample 2 at $T = 300$ K and $H = 350$ Oe. (a) SDM ($I = 0.78$ mA), and (b) FMM ($I = 1.15$ mA). (c) Average residual time as a function of current. The lines in (c) are obtained from the theory ((1)).

(~ 0.86 mA at $H = 350$ Oe. H_c of sample 2 is 550 Oe) in the SDM. The absence of telegraph noise at $I > I_c$ is due to the single energy minimum in region II when the magnetizations are in the single domain state. In the FMM, however, we observed telegraph noise although the current is larger than the critical value (figures 4(b) and (c)). For a given applied field ($H = 350$ Oe) the average residual time (τ_{AVE}) at $\tau_P = \tau_{AP}$ in the SDM (~ 1.3 μ s) is 20 times larger than that in the FMM (~ 0.063 μ s), indicating that the effective value of $(E_B/k_B T)_{SDM}$ is three times ($\sim \ln(20)$) larger than $(E_B/k_B T)_{FMM}$. When we follow the concept of the effective magnetic temperature model, the magnetic temperature in this case is about 600 K. However, the effective magnetic temperature model cannot explain why the number of energy minima changes from 1 to 2 due to the incoherence spin-wave.

A plausible way of explaining the telegraph noise in region II is to replace I_c^{SDM} by an effective I_c^{FMM} (4) [15]:

$$I_c^{FMM} = \frac{2\gamma e S \alpha}{P} \left(H + H_K + 2\pi M_s + \frac{2\pi^2 D}{\mu_B \lambda(I)^2} \right) \quad (4)$$

where D is the spin-stiffness constant and $\lambda(I)$ is the wavelength of the spin-wave which is function of the current. The experimental results on telegraph noise of [20] can be understood in terms of the excitation of an incoherent spin-wave.

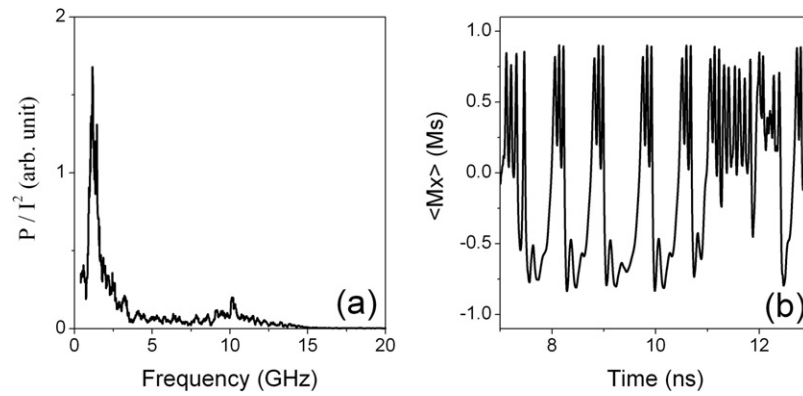


Figure 5. (a) Power spectrum and (b) telegraph noise (sample 1, $I = 7$ mA, $H = 400$ Oe, and $T = 0$ K) [31].

3.3. Telegraph noise in region IV ($I > I_c$ and $H > H_c$) [31]

The incoherence significantly changes the feature of the telegraph noise and yields telegraph noise even in region IV. In the coherent spin-torque model, a random jump between P and AP states is not allowed at zero temperature since there is no activation energy (see (1)). When the magnetic dynamics is incoherent, however, the energy of the spin-wave can be a new source of activation energy and it eventually yields the telegraph noise.

Figure 5 shows a power spectrum and telegraph noise with a gigahertz frequency obtained at zero temperature. An interesting feature in the spectrum of figure 5(a) is that the largest peak is obtained at 1 GHz. The spectrum obtained from the FMM almost duplicates the reported experimental result [19]. Such a low-frequency peak is rather surprising because the actual precession frequency of local magnetization induced by the STT is of about 10 GHz (see the smaller and broader peak in the spectrum around 10 GHz in figure 5(a)). As shown in figure 5(b), the unexpected low-frequency dynamics corresponds to random jumps between almost P and AP magnetic configurations. In the random fluctuation patterns, the dynamics of the P state is quite different from that of the AP state. This is because the instabilities in the former and latter states are respectively driven by the STT (spin-waves) and the external field (no spin-wave). More importantly, it should be noted that the telegraph noise was obtained using zero-temperature calculations at $H > H_c$ [31]. This simulation result proves that the incoherent spin-wave excitation results in telegraph noise at the bias condition of $I > I_c$ and $H > H_c$. This simulation result explains the experimental results on gigahertz telegraph noise of [22] in terms of the excitation of an incoherent spin-wave.

3.4. Effects of the incoherent spin-wave excitation on the switching current and time [32]

An attractive theoretical prediction of the current-induced magnetization switching is a very weak dependence of the critical current density (J_c) on a possible distribution of cell size. This is because J_c is proportional to $(2\pi M_s + H_c)$, where M_s is the saturation magnetization and H_c is the coercivity of the free layer. H_c is sensitive to the cell size but is much smaller than $2\pi M_s$. A very weak cell-size dependence of J_c is crucial for a mass production of such devices. However, micromagnetic simulations have revealed that the magnetic dynamics induced by the spin-transfer torque in a nanopillar could be highly nonlinear. Therefore, the prediction from the single domain spin-torque theory should be rigorously tested in the framework of

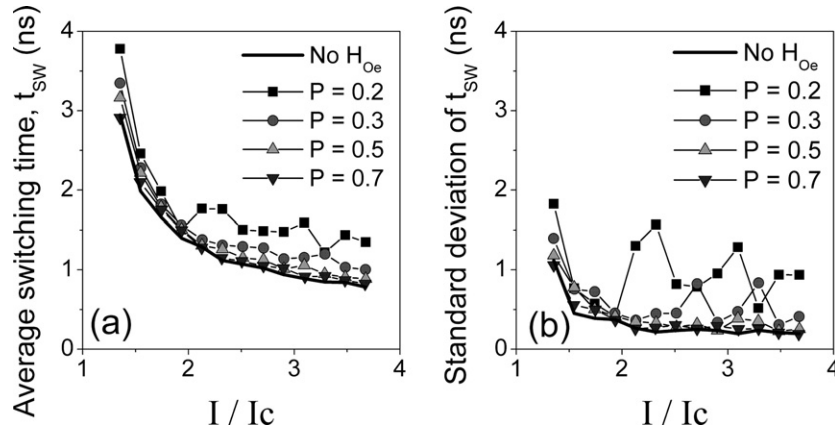


Figure 6. Average and standard deviation of switching time as a function of current for various spin polarization factors [32], P ; (a) average, and (b) standard deviation (cell size = $120 \times 56 \text{ nm}^2$). I_c is the theoretical critical current for the onset of magnetic excitations.

micromagnetics. In this section, we briefly give an overview of the influence of magnetic cell size and spin polarization on the switching current density and switching as reported in [32].

The average (t_{SW}) and the standard deviation of the switching time as a function of the current (I) were calculated for various spin polarization factors, P (figure 6, sample size = $120 \times 56 \text{ nm}^2$, elliptical shape). All switching events have been calculated at room temperature (RT). The average switching time and standard deviation were statistically analysed from an ensemble consisting of 100 switching events. Without considering the current-induced magnetic field (Oersted field, H_{Oe}), a monotonic decay of t_{SW} with current is observed. It shows an inverse proportionality to $(I - I_c)$ as predicted by the macrospin model [5], where I_c is the theoretical critical current for the onset of magnetic excitations. When H_{Oe} is taken into account, however, the dependence of t_{SW} on current dramatically changes. It can even become non-monotonic (for instance, $P = 0.2$ in figure 6(a)) and exhibits a kink as experimentally observed by Emley *et al* [37]. The standard deviation also increases for currents larger than the critical value for the kink (figure 6(b)). In this tested sample, the switching is delayed over the full investigated range of current when taking into account H_{Oe} . We found that the retardation is caused by vortex formation during the switching. Note that the kink disappears when P is sufficiently large ($P = 0.7$, figure 6(a)). This indicates that the kink is caused by the circular Oersted field which results in the excitation of an incoherent spin-wave including the dynamic vortex. However, when the spin-transfer torque is much larger than that due to H_{Oe} , the incoherence is suppressed and the magnetic dynamics recovers a single-domain-like behaviour.

We studied the probability of switching (P_{SW}) as a function of pulsed current for various aspect ratios and cell areas (figure 7). For $P = 0.2$, we observed a difference in the distributions of P_{SW} with varying aspect ratio (AR). More importantly, the switching probability never reached 100% at high currents due to vortex formation (figure 7(a)). For $P = 0.7$, however, the distributions of P_{SW} are almost identical and the magnetization completely switches for all switching events at high enough currents (figure 7(b)). When the size of the cell ($L \times W$; L and W are the lengths of the magnetic cell along the in-plane long axis and the in-plane short axis, respectively) is smaller than 100 nm (AR = 2.0), almost identical distributions of P_{SW} were obtained for both low ($P = 0.2$) and high ($P = 0.7$) spin polarization (figures 7(c) and (d)).

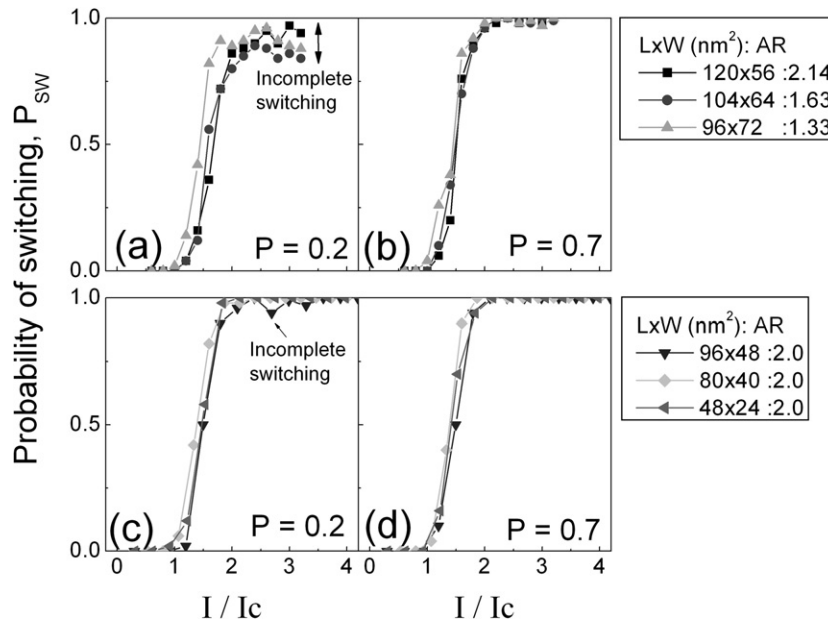


Figure 7. Probability of switching as a function of current [32]. Constant cell area: (a) $P = 0.2$, and (b) $P = 0.7$. Constant aspect ratio: (c) $P = 0.2$, and (d) $P = 0.7$.

An exceptional case is for $P = 0.2$ and $(L \times W) = (96 \times 48 \text{ nm}^2)$ where a few incomplete switchings due to vortex formation were still observed.

4. Limitations and perspectives of micromagnetic modelling on the current-induced magnetization dynamics

In this section, we discuss the limitations of our micromagnetic modelling on the current-induced magnetization dynamics. We also discuss which parts in the modelling should be modified and be improved in future work.

In this work, we took the simplest forms of important parameters, for instance, no angular dependence of the spin torque, because the magnetization dynamics even with the simplest forms is already very complex to understand. Our work is still valuable for obtaining the general idea of the current-induced magnetization dynamics even though we did not consider the parameters in a more correct way. However, it is evident that a rigorous consideration of the parameters enables us to accurately describe the current-induced dynamics.

From this viewpoint, an important parameter is the Gilbert damping. In this work we assumed a constant value of the Gilbert damping constant. However, dissipation mechanisms are not well understood in these systems even though they play very important roles in the current-driven dynamics and thermal fluctuations. The simplified Gilbert damping would not be proper for describing effective damping in many aspects. For instance it may be a tensor [38]. Spatially non-uniform enhancement of the damping due to the eddy current may not be negligible. There should be an enhancement of the Gilbert damping due to the spin pumping [39]. Furthermore, it is angularly dependent in a spin valve structure [40] and affects the current-induced magnetization dynamics [41].

More importantly, the Slonczewski torque terms were originally suggested within the context of uniform precessional dynamics. In this work, we have extended this model to go

beyond the restriction by allowing the magnetization to vary spatially. Therefore corrections due to the feedback between the in-plane inhomogeneous magnetization and the spin torque should be taken into account. We did not self-consistently calculate the current density in this work. We investigated the effect of the in-plane inhomogeneous magnetizations on the in-plane distribution of the *charge* current (not shown). This could be important because the magnetoresistance (MR) is a function of the angle between two magnetizations (free and pinned layers). We found that it is negligible in a fully metallic spin valve studied in this work because of the small change in MR (\sim a few %). However, it can be significant in a sample including a tunnel barrier with a big MR.

Although the effect of the inhomogeneous magnetizations on the *charge* current is negligible in a fully metallic sample, on the *spin* current it is significant. To properly take into account the feedback between the inhomogeneous magnetizations and the spin torque, we have to self-consistently solve both the Landau–Lifshitz–Gilbert equation and the equation of motion of the spin accumulation coupled with the spin current. All the above factors should be included or be modified for a better understanding of the current-induced magnetization dynamics.

5. Conclusion

The experimental results on telegraph noise can now be explained in a unified way by the excitation of incoherent spin-waves at $I > I_T$. The controversy about the fact that the experimental results were supporting one or other model (the coherent spin-torque model [13, 24] or the effective magnetic temperature model [20–22]) was due to the telegraph noise being measured within different ranges of current where one or the other model seems valid. From this study, we can conclude that both the coherent spin-torque model and the effective magnetic temperature model can be unified in a single concept, the difference in incoherent spin-wave excitations depending on the current. Our approach based on the full micromagnetic LLG equation modified by the spin-torque term allows covering all ranges of currents.

Magnetic dynamics excited by spin current in nanopillars can be incoherent, depending on the injected current. This phenomenon is mainly due to the spatial inhomogeneities of the circular magnetic field (H_{Oe}), which generate a distribution of local precession frequencies. We could explain inconsistencies between the coherent spin-torque model and the effective temperature model by using the incoherent spin-wave excitations. The telegraph noise can be observed at three different bias conditions ((1): $I < I_c$ & $H < H_c$, (2): $I > I_c$ & $H < H_c$, and (3): $I > I_c$ & $H > H_c$) due to the incoherent spin-waves.

Because the circular magnetic field (H_{Oe}) is the main origin of the incoherence, the cell size can significantly affect the switching statistics. The increase in the spin polarization and/or the reduction in the cell size are essential not only for reducing the switching current density but also for controlling the switching current and pulse width within acceptable margins.

Acknowledgments

We thank B Dieny, A Vedyayev, U Ebels, and I N Krivorotov for fruitful discussions. Financial support from the National Research Laboratory program is gratefully acknowledged.

References

- [1] Slonczewski J C 1996 *J. Magn. Magn. Mater.* **159** L1
- [2] Berger L 1996 *Phys. Rev. B* **54** 9353

- [3] Bazaliy Y B, Jones B A and Zhang S C 1998 *Phys. Rev. B* **57** R3213
- [4] Stiles M D and Zhangwill A 2002 *Phys. Rev. B* **66** 014497
- [5] Sun J Z 2000 *Phys. Rev. B* **62** 570
- [6] Wegrowe J E 2000 *Phys. Rev. B* **62** 1067
- [7] Zhang S, Levi P M and Fert A 2002 *Phys. Rev. Lett.* **88** 236601
- [8] Tsoi M, Jansen A G M, Bass J, Chiang W C, Seck M, Tsoi V and Wyder P 1998 *Phys. Rev. Lett.* **80** 4281
- [9] Myers E M, Ralph D C, Katine J A, Louie R N and Buhrman R A 1999 *Science* **285** 867
- [10] Tsoi M, Jansen A G M, Bass J, Chiang W C, Tsoi V and Wyder P 2000 *Nature* **406** 46
- [11] Katine J A, Albert F J, Buhrman R A, Myers E B and Ralph D C 2000 *Phys. Rev. Lett.* **84** 4212
- [12] Myers E B, Albert F J, Sankey J C, Bonet E, Buhrman R A and Ralph D C 2002 *Phys. Rev. Lett.* **89** 196801
- [13] Albert F J, Emley N C, Myers E B, Ralph D C and Buhrman R A 2002 *Phys. Rev. Lett.* **89** 226802
- [14] Grollier J, Boulenc P, Cros V, Hamzić A, Vaurès A and Fert A 2001 *Appl. Phys. Lett.* **78** 3663
- [15] Sun J Z, Monsma D J, Kuan T S, Rooks M J, Abraham D W, Oezylmaz B, Kent A D and Koch R H 2003 *J. Appl. Phys.* **93** 6859
- [16] Lee K J, Liu Y, Deac A, Li M, Change J W, Liao S, Ju K, Redon O, Nozières J P and Diény B 2004 *J. Appl. Phys.* **95** 7423
- [17] Tulapurkar A A, Devolder T, Yagami K, Crozat P, Chappert C, Fukushima A and Suzuki Y 2004 *Appl. Phys. Lett.* **85** 5358
- [18] Devolder T, Crozat P, Kim J V, Chappert C, Ito K, Katine J A and Carey M J 2006 *Appl. Phys. Lett.* **88** 152502
- [19] Kiselev S I, Sankey J C, Krivorotov I N, Emley N C, Schoelkopf R J, Buhrman R A and Ralph D C 2003 *Nature* **425** 380
- [20] Urazhdin S, Birge N O, Pratt W P and Bass J 2003 *Phys. Rev. Lett.* **91** 146803
- [21] Fábíán A, Terrier C, Guisam S S, Hoffer X, Dubey M, Gravier L and Ansermet J P 2003 *Phys. Rev. Lett.* **91** 257209
- [22] Pufall M R, Rippard W H, Kaka S, Russek S E and Silva T J 2004 *Phys. Rev. B* **69** 214409
- [23] Rippard W H, Pufall M R, Kaka S, Russek S E and Silva T J 2004 *Phys. Rev. Lett.* **92** 027201
- [24] Krivorotov I N, Emley N C, Garcia A G F, Sankey J C, Kiselev S I, Ralph D C and Buhrman R A 2004 *Phys. Rev. Lett.* **93** 166603
- [25] Li Z and Zhang S 2003 *Phys. Rev. B* **68** 024404
- [26] Li Z and Zhang S 2004 *Phys. Rev. B* **69** 134416
- [27] Wegrowe J E, Hoffer X, Guittienne P, Fábíán A, Gravier L, Wade T and Ansermet J P 2002 *J. Appl. Phys.* **91** 6806
- [28] Urazhdin S 2004 *Phys. Rev. B* **69** 134430
- [29] Miltat J, Albuquerque G, Thiaville A and Vouille C 2001 *J. Appl. Phys.* **89** 6982
- [30] Zhu J G and Zhu X C 2004 *IEEE Trans. Magn.* **40** 182
- [31] Lee K J, Deac A, Redon O, Nozières J P and Diény B 2004 *Nat. Mater.* **3** 877
- [32] Lee K J and Diény B 2006 *Appl. Phys. Lett.* **88** 132506
- [33] Brown W F 1979 *IEEE Trans. Magn.* **15** 1196
- [34] Barnes S E 2006 *Phys. Rev. Lett.* **96** 189701
- [35] Tataru G and Kohno H 2006 *Phys. Rev. Lett.* **96** 189702
- [36] Acremann Y, Strachan J P, Chembrolu V, Andrews S D, Tyliszczak T, Katine J A, Carey M J, Clemens B M, Siegmann H C and Stöhr 2006 *Phys. Rev. Lett.* **96** 127202
- [37] Emley N C, Krivorotov I N, Sankey J C, Ralph D C and Buhrman R A 2004 *49th MMM Conf. (Jacksonville, USA)* HA-14
- [38] Safonov V L 2002 *J. Appl. Phys.* **91** 8653
- [39] Terkovnyak Y, Brataas A and Bauer G E 2002 *Phys. Rev. Lett.* **88** 117601
- [40] Terkovnyak Y, Brataas A and Bauer G E 2003 *Phys. Rev. B* **67** 140404
- [41] Kim W J, Lee T D and Lee K J 2006 *IEEE Trans. Magn.* **42** 3207